In-situ Film Growth of Metallo-Supramolecular Polymer *via* Electropolymerization and Its Application as Electrochromic Film

Chih-Wei Hu, Satya Ranjan Jena, Takashi Sato, Jian Zhang, Satoshi Moriyama, Masayoshi Higuchi*

Electronic Functional Macromolecules Group, National Institute for Materials Science (NIMS), 1-1 Namiki, Tsukuba 305-0044, Japan, Email: higuchi.masayoshi@nims.go.jp

ABSTRACT: Electropolymerization is an important technique for surface functionalization owing to its convenient and controlled synthetic pathways. The in-situ synthesis of metallo-supramolecular polymers (MSPs) utilizing coordination-driven metal ions and coordinating ligands as well as studying their potential applications using electropolymerization have been less explored. Herein, we demonstrated the formation of MSPs on a pre-terpyridine-functionalized indium tin oxide (ITO) glass substrate by using Fe(III) ions and 4′,4′′′′-(1,4-phenylene)-bis(2,2′:6′,2′′-terpyridine) ligand. By providing an anodic potential, polymer growth occurred due to the strong coordination between the reduced metal ions (Fe(II)) and the bis-terpyridine ligand. The formation of the polymer was evident from the growth of the corresponding peaks in the cyclic voltammogram and UV-vis spectral profile. The surface morphology was characterized using atomic force microscopy (AFM). The electrochromic (EC) properties of the electropolymerized MSP (EP-MSP) were studied by utilizing the metal-to-ligand charge-transfer color band of the redox-active Fe(II)-(terpyridine)$_2$ unit present in the MSP backbone. It was observed that the film exhibited an optical switching coloring time of 2.1 s and 5.7 s for bleaching, a transmittance change of 54%, and a coloration efficiency of 142.6 cm^2 C^{-1}.

KEYWORDS: *Electropolymerization, Metallo-supramolecular polymers, Electrochromic, Coloration efficiency, Switching time, Optical contrast.*

1. INTRODUCTION

Surface functionalization is of immense importance in the field of materials science because of its potential applications. There is high demand for surface-based controlled synthesis of functional conductive polymers because these polymers exhibit strong electron mobility inside the macrocyclic architecture, quick electrochemical switching, and superior thermal and chemical durability.[1] Several methods have been implemented to functionalize conductive surfaces; however, electropolymerization is the oldest, quickest, and most convenient technique. It has many advantages over conventional polymerization techniques, including the ability to control the thickness and properties of the polymer film, as well as single-step synthetic procedures.[2] This technique is especially suitable for the preparation of conductive polymers, including poly(3,4-ethylenedioxythiophene),[3] polyaniline,[4] polypyrrol,[5] and polythiophene,[6] as well as for the synthesis of transition metal complex materials (e.g., Prussian blue).[7] The active unit of the polymer backbone allows the functionalized surface to be used for various applications,[8] such as organic light-emitting diodes (OLEDs),[9] sensing,[10] energy storage devices (such as batteries and supercapacitors),[2,11–13] organic solar cells,[14] chemical separations, electrochromic devices,[15] electrocatalysts,[16] and biomedical applications.[17]

Three methods have been mainly used for the in-situ film preparation of metallo-supramolecular polymers (MSPs) on a substrate: coordinative assembly of metal ions to an organic polymer film,[18,19] layer-by-layer (LbL) electrostatic deposition,[20–23] and electropolymerization.[24,25] This coordinative assembly was investigated in detail by Tieke and co-workers.[26–28] Organic polymers with coordination sites on their side chains were used. MSP films were obtained by assembling metal ions (Co^{2+}, Ni^{2+}, and Zn^{2+}) into organic polymer films through complexation with the coordination sites. The resulting polymer thin films exhibited multicolor electrochromic (EC) properties and a special redox reaction mechanism. Several researchers have reported on the LbL deposition method. Pan *et al.* used terpyridine-modified multiwalled carbon nanotubes and ruthenium(III) ions to form an LbL structure.[29] Liu *et al*. used viologen thiol-functionalized carbon nanotube and Cu^{2+} to obtain an LbL-deposited hybrid film that exhibited novel electrochemical properties.[30] On the other hand, Zacher *et al*. also summarized the metal-organic framework structures formed via LbL deposition.[31,32] However, LbL deposition techniques are typically cumbersome and time-consuming, necessitating changes in the electropolymerization techniques. The complex monomer can be polymerized on a conductive surface using an electroactive polymerizable unit, such as vinyl, thiophene, pyrene, triphenylamine, or carbazole.[33] Several polymerizable units resulting from oxidative electropolymerization via the formation of radical cations have been explored by Schubert et al.[34] Similarly, Nie et al. showed that the formation of radical anion intermediates led to reductive polymerization of different vinyl-substituted polypyridyl complexes.[35] Hanabusa *et al*. electropolymerized a bis[2-(hydroxyphenyl)-2,2':6,2"-terpyridinyl](M^{2+}) (M: Fe and Ru) series, which showed special electrochromic and photocurrent response.[36] However, reports on the in-situ formation of MSPs on surfaces via metal ions and coordinating ligands by electropolymerization are rare. Toma et al. reported the preparation of coordinative polymers by electropolymerization.[37] They used a triruthenium cluster and Fe^{3+} ions to form a stable surface on Fluorine-doped Tin Oxide (FTO) glass. However, the applications of such electropolymerized MSP (EP-MSP)-thin films have not yet been discussed in the literature. Herein, we report the in-situ synthesis of an EP-MSP-thin film on a transparent conductive substrate (Indium Tin Oxide (ITO) glass) using Fe^{3+} ions and a bis-terpyridine ligand. Additionally, the electrochromic properties, including optical contrast, response time, and coloration efficiency, of EP-MSP were investigated.

2. EXPERIMENTAL SECTION

2.1. Materials and analytical techniques

All the chemicals were purchased from Sigma-Aldrich Pvt. Ltd. and Tokyo Chemical Industry Co., Ltd. and used without further purification. Acetonitrile (ACN) and dimethyl sulfoxide (DMSO) were used as analytical grade electropolymerization solvents. UV-vis spectra were obtained using an ocean optical light source (DH-2000) and a spectrophotometer (USB4000). 4′,4′′′′-(1,4-Phenylene)bis(2,2′:6′,2′′-terpyridine) (**L1**) was purchased from Sigma-Aldrich Pvt. Ltd. (97% purity) and used directly without further purification. **L2** was synthesized according to a previously reported method.[37] Cyclic voltammetry (CV) and chronoamperometry experiments were performed in an argon-saturated anhydrous ACN solution containing 0.1 M $LiClO_4$ as the supporting electrolyte using an electrochemical analyzer (ALS/CH instruments). Atomic force microscopy (AFM) measurements were conducted using a Seiko Instruments Inc. (SII) atomic force microscope (NanoNavi II) in the dynamic force mode (DFM) at a scan rate of 1.0 Hz in air at room temperature(25 °C).

All the MSP films for electrochemical analysis were prepared via electropolymerization using an indium tin oxide (ITO)-coated glass slide as the working electrode (slide area of 1 × 4 cm^2).

2.2. Electroplating solution

The electroplating solution was composed of two solvents: ACN and DMSO in a volume ratio of 10:1. $FeCl_3$ (1 mM) was dissolved in ACN, and the solution was labelled as solution [A]. **L1** (10 mM) was dissolved in DMSO and labelled as solution [B]. Solution [A] was light orange, and solution [B] was white and milk-like. Before electropolymerization, a volume ratio of 10:1 of [A]:[B] was added to the electrochemical reactor. The electroplating solution contained equal molar amounts of Fe^{3+} and **L1**.

2.3. Electropolymerization process

Initially, the ITO substrate was functionalized with 0.001 M **L2** solution. A three-electrode setup consisting of the pre-functionalized ITO glass was used as the working electrode with a working area of 1 × 1 cm^2; a platinum wire was used as the counter electrode; and a homemade Ag/Ag^+ in ACN with 0.1 M tetrabutylammonium perchlorate (TBAP) and 0.01 M $AgNO_3$ was used as the reference electrode. By mixing the calculated amounts of solutions [A] and [B] into the electrochemical reactor, we used CV and chronoamperometry techniques to deposit EP-MSP films on ITO glass. After electropolymerization, a dry ACN solution was used to wash the ITO surface, and the electrode was stored in air.

The expected MSP structure consists of Fe^{2+} ions, the connecting ligand between the metal ions:4′,4′′′′-(1,4-phenylene)-bis(2,2′:6′,2′′-terpyridine) (**L1**), and the "bridging ligand with the metal ion and ITO surface":4′-(4-(2-(triethoxysilyl)vinyl)phenyl)-2,2′:6′,2′′-terpyridine (**L2**). The electropolymerization mechanism is illustrated in Figure 1. When Fe^{3+} was electrochemically reduced to Fe^{2+} by applying a negative potential to the working ITO electrode, we expected that an MSP film would be formed owing to the strong binding affinity of the terpyridine moiety to the reduced Fe^{2+} ion.

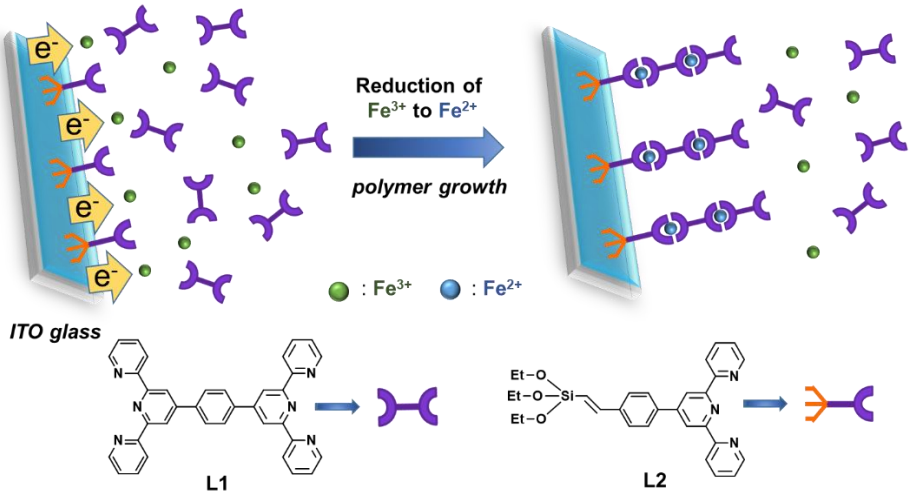

Figure 1. Schematic of the synthesis of electropolymerized MSP (EP-MSP)-thin film containing Fe^{2+} ions, a "connecting ligand" (L1), and a "bridging ligand" (L2) on an ITO glass

3. RESULTS AND DISCUSSION

3.1. Electropolymerization of MSP

CV and chronoamperometry were used for electrochemical polymerization. (Figure 1). The ITO substrate was first treated with **L2** and then subjected to deposition using a three-electrode setup. The scanning potential was 0 to −1.5 V, increased to +1.5 V, and then finally decreased to 0 V for a complete cycle. Electropolymerization was performed for 20 cycles at a scan rate of 100 mV s^{-1}. In the first cycle, two redox pairs were observed at a peak potential (E_P) of −0.49 V and +0.86 V. The anodic redox pair was due to the redox reaction of Fe^{3+}/Fe^{2+} ions on the ITO glass. Although the ITO surface was treated with **L2** in advance, the surface area may not have been fully covered by **L2**, thus providing a reaction point for the Fe^{3+}/Fe^{2+} ions. The cathodic redox pair was due to the $Fe^{2+}(tpy)_2$ redox center of EP-MSP thin film, which exhibited a narrow peak separation of 0.27 V at the first cycle. The anodic redox wave began to

disappear as the cycle number increased (1 to 20), whereas the cathodic wave intensified. The saturation of the Fe^{3+}/Fe^{2+} ion redox pair might be attributed to the reduction in ion diffusion from the bulk to the electrode surface owing to the formation of the MSP chain.[37,38] This phenomenon demonstrated the effectiveness of electropolymerization for polymer growth. Owing to the consistent growth of the EP-MSP thin film throughout the cycles, the CV area of the cathodic potential redox waves gradually increased at the same time. The electropolymerization CV profile of the bare ITO glass without **L2** modification is presented in the inset of Figure 1. The results demonstrated that only a small CV area increased in the positive potential range, and the redox pair of Fe^{3+}/Fe^{2+} ions was seldom altered in the negative potential range. Although some EP-MSP thin films were still deposited on the ITO surfaces, their poor adherence caused them to collapse into the solution.

3.2. UV-vis and cyclic voltammogram analysis

The electropolymerization of the EP-MSP thin film was also confirmed by chronoamperometry. The potential was set at −1.5 V for different deposition times (100–2500 s). The *in-situ* absorbance changes during electropolymerization are shown in Figure 2b. The electroplating solution was initially transparent and light purple (0 s), exhibiting an absorption maximum (λ_{max}) at 578 nm. The absorbance peak at 0 s may result from a weak binding force between the relatively rare Fe^{2+} and **L1** in the electroplating solution, which could be triggered by the spontaneous conversion of Fe^{3+} to Fe^{2+}. The increased absorbance at 578 nm, which was proportional to the deposition time, confirmed that the EP-MSP coating had formed on the ITO glass. The absorbance peak at 578 nm was attributed to metal-to-ligand charge transfer (MLCT) from the coordination of Fe^{2+} ions with the terpyridine unit of **L1**. The increase in absorbance was due to the growth of MSP chains on the ITO surface. CV profile of the EP-MSP film exhibited a clear redox peak potential (E_p) at +0.76 mV (*vs.* Ag/Ag^+) in 0.1 M $LiClO_4$/ACN electrolyte solution with a scan rate of 20 mV s^{-1} (Figure 2C). The peak separation (ΔE_p) between the oxidation and reduction peaks was of 140 mV, which was higher than that reported in our previous study, in which a chemically polymerized MSP (CP-MSP) exhibited a ΔE_p of 27 mV.[39] This larger separation may be due to the longer electron-transfer length of bridging ligand **L2**.[40] Furthermore, the inflexible linear structure of EP-MSP hindered electron transfer by the inter-polymer chains. A linear relationship between the peak current and scan rate was observed in the CV plots of the EP-MSP film at various scan rates (Figure 2D and S1). This outcome indicates a kinetically controlled reaction for the surface-bound EP-MSP thin film but not a diffusion-controlled reaction, probably due to the low conductivity of the rigid polymer film.

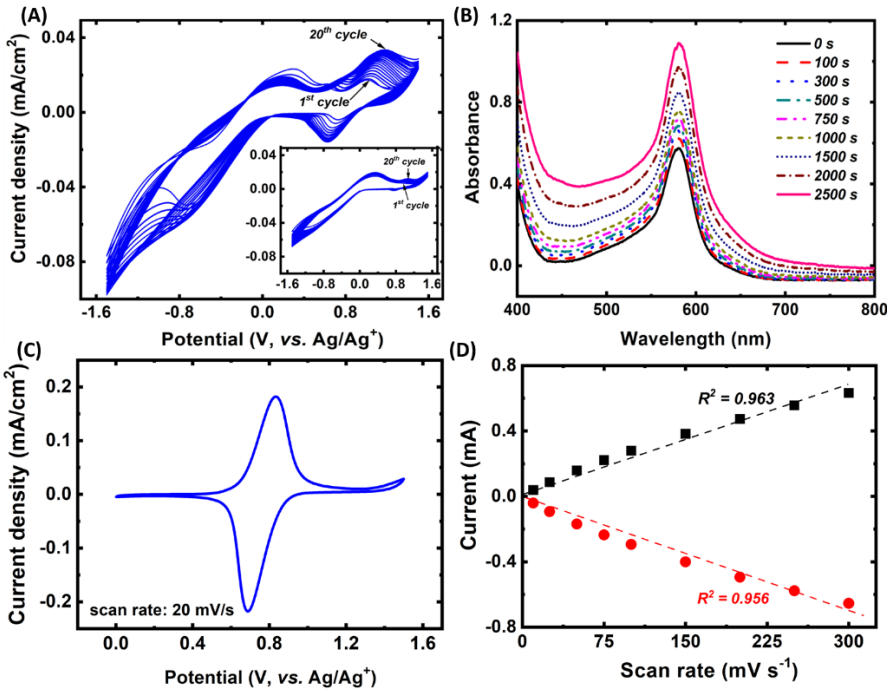

Figure 2. (A) Cyclic voltammograms (CVs) of the **L2**-modified ITO glass during electropolymerization for the first 20 cycles at a scan rate of 100 mV s^{-1}. Inset: CVs of an EP-MSP film obtained on an ITO glass without the treatment with **L2**. (B) UV-vis spectral monitoring for in-situ EP-MSP film growth by setting a potential at -1.5 V at different deposition times (100–2500 s). (C) CV of the polymer film (electrolyte: 0.1 M $LiClO_4$/acetonitrile; scan rate: 20 mV s^{-1}). (D) Relationship between the cathodic peak current (I_{pc}; black) and anodic peak current (I_{pc}; red) with scan rate.

3.3. Surface morphology of the EP-MSP film

The AFM images of the EP-MSP films were obtained by performing chronoamperometry at different times (Figure 3). Compared to the CP-MSP film (Figure S2), the EP-MSP film (Figure 3A,B) exhibited a much more fiber-like structure, and each branch was constructed with many spherical polymers. These small round polymers had an average diameter of 100 nm. We proposed that polymer chains were formed by sequentially connecting these spherical polymers and extending their chain lengths from the ITO surface. Many empty areas were observed between the polymer chains (dark areas in Figure 3B). The

images further indicated that the growth mechanism was consistent with our mechanistic illustration, which showed that the polymer chains grew from the bottom surface to the top. The thicker EP-MSP film was obtained at a constant voltage of −1.5 V applied for 2000 s (Figure 3C,D). Some polymers appeared to partially agglomerate at the surface, and all the distances between the polymeric chains were estimated. The change in the morphology could result from the overexpanded polymer chains becoming heavily entangled, which causes an accumulation of electropolymerized polymers on the surface.

3.4. Electrochromic and electrochemical properties of the EP-MSP film

The EP-MSP cathodically colored the EC material, because the absorbance decreased with increased oxidative potentials. In the absorbance spectra of the EP-MSP film at different potentials, the absorption peak at 578 nm started to decrease at +0.6 V due to the oxidation of Fe^{2+} to Fe^{3+} and the MLCT. The peak completely vanished at +1.0 V (Figure 4A). The change in transmittance (ΔT%) at 578 nm in the EP-MSP film that switched between 0 and +1.2 V with an interval time of 10 s was 54.4%. The coloring time (t_c) was calculated to be 2.1 s, whereas the bleaching time (t_b) was 5.7 s (switching time was the time needed for 95% change of ΔT) (Figure 4B). This implies that the bleached state was more unstable than the colored state in the EP-MSP film, as the oxidized states lacked electrons because t_c was lesser than t_b. Using the chronoamperometry plot (Figure 4C), the total charge consumed by the EP-MSP film was calculated by integrating the current area. It showed the charge consumed at oxidation was 1.83 mC cm^{-2} while the charge released during reduction was 2.79 mC cm^{-2}. A good EC material consumes less charge with high optical change, and the relationship is described as "coloration efficiency." The coloration efficiency (η) of EP-MSP thin film was calculated to be 142.6 cm^2 C^{-1} at 578 nm. The photographic color changes are shown in Figure 4D.

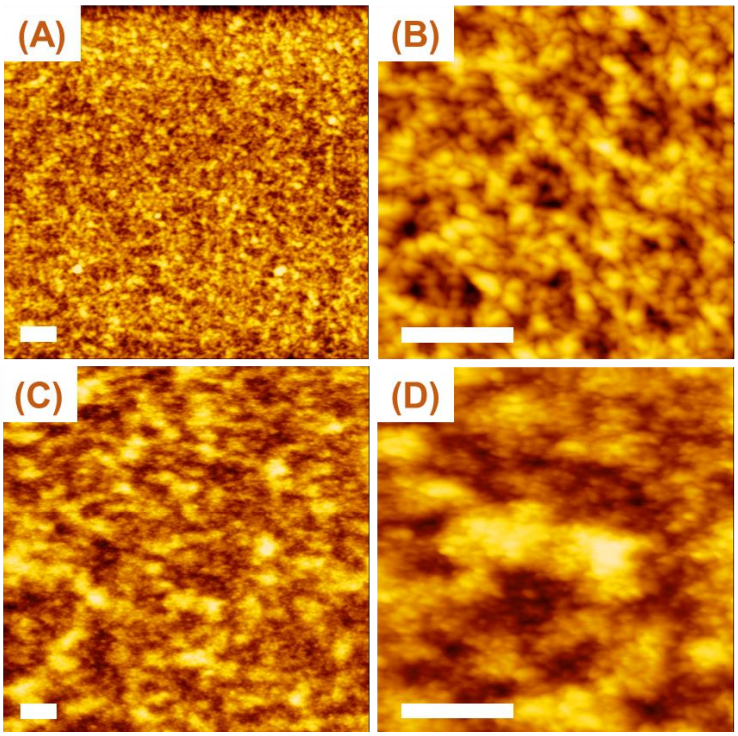

Figure 3. (A, B) AFM images of the EP-MSP film obtained at a constant voltage of −1.5 V for 300 s. (C, D) The surface morphology of the EP-MSP film obtained at a constant voltage of −1.5 V for 2000 s. All the scale bars were equal to 500 nm.

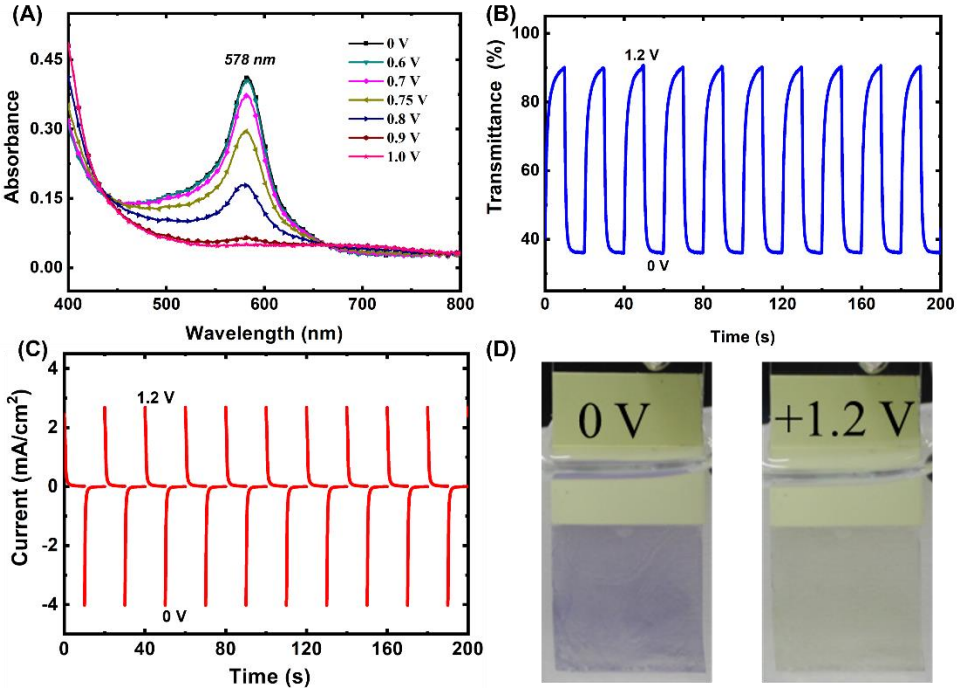

Figure 4. (A) In-situ UV-vis spectra of EP-MSP film in a 0.1 M $LiClO_4$/ACN solution at different applied potentials. (B) Transmittance change (ΔT, %) at 578 nm of EP-MSP film switched between 0 and +1.2 V in 0.1 M $LiClO_4$/ACN with an interval time of 10 s. (C) In-situ current response in the EP-MSP film when switching between 0 and 1.2 V.(D) Digital pictures of EP-MSP film color switching.

4. CONCLUSION

In this study, we demonstrated the synthesis of (EP-MSP) thin films on ITO glass by in-situ electropolymerization. The electrochemical properties, surface morphologies, and EC conductivity of the EC films were also investigated. To the best of our knowledge, this is the first report on the application of in-situ-synthesized EP-MSP thin films for EC applications. The growth of the EP-MSP film was clearly observed via CV and UV-vis. The polymers exhibited a stable growth by applying a constant voltage of −1.5 V from 300 s to 2000 s. The EP-MSP film exhibited a color transition from blue to transparent for the voltage range of 0 V to 1.2 V, respectively. The t_c (2.1 s) was shorter than the t_b (5.7 s) because of the formation of an unstable Fe(III) state during bleaching. In addition, the film exhibited a high ΔT (54.4% at 578 nm), high coloration efficiency (142.6 $cm^2\ C^{-1}$ at 578 nm), and unique surface morphologies. We believe that in-situ fast electropolymerized synthesis techniques will pave the way for investigating several other material chemistry applications.

ASSOCIATED CONTENT

SUPPORTING INFORMATION

Additional experimental details related to this article, containing additional figures, can be found in the online version. This material is available free of charge via the Internet at http://pubs.acs.org.

AUTHOR INFORMATION

Corresponding Author

Masayoshi Higuchi − Electronic Functional Macromolecules Group, National Institute for Materials Science (NIMS), 1-1 Namiki, Tsukuba 305-0044, Japan; E-mail: higuchi.masayoshi@nims.go.jp

Authors

Chih-Wei Hu − Electronic Functional Macromolecules Group, National Institute for Materials Science (NIMS), 1-1 Namiki, Tsukuba 305-0044, Japan

Satya Ranjan Jena − Electronic Functional Macromolecules Group, National Institute for Materials Science (NIMS), 1-1 Namiki, Tsukuba 305-0044, Japan

Takashi Sato − Electronic Functional Macromolecules Group, National Institute for Materials Science (NIMS), 1-1 Namiki, Tsukuba 305-0044, Japan

Satoshi Moriyama − Electronic Functional Macromolecules Group, National Institute for Materials Science (NIMS), 1-1 Namiki, Tsukuba 305-0044, Japan

The authors declare no conflicts of interest.

ACKNOWLEDGMENTS

This research work was financially supported by the Mirai project (grant number: JPMJMI21I4) from the Japan Science and Technology Agency (JST) and the Environment Research and Technology Development Fund (ERTDF) (JPMEERF20221M02) from Environmental Restoration and Conservation Agency (ERCA).

REFERENCES

(1) Her, L.-J.; Hong, J.-L.; Chang, C.-C. Preparation and Electrochemical Characterizations of Poly(3,4-Dioxyethylenethiophene)/$LiCoO_2$–Ketjenblack Composite Cathode in Lithium-Ion Battery. *J. Power Sources* **2006**, *161*, 1247–1253.

(2) Zhang, C.-X.; Mei, S.-L.; Chen, X.-H.; Liu, E.-T.; Yao, C.-J. Electrochemical Construction of Functional Polymers and Their

Application Advances in Lithium Batteries. *J. Mater. Chem. C* **2021**, *9*, 17182–17200.

(3) Pringle, J. M.; Armel, V.; MacFarlane, D. R. Electrodeposited PEDOT-on-Plastic Cathodes for Dye-Sensitized Solar Cells. *Chem. Commun.* **2010**, *46*, 5367–5369.

(4) Gospodinova, N.; Terlemezyan, L. Conducting Polymers Prepared by Oxidative Polymerization: Polyaniline. *Prog. Polym. Sci.* **1998**, *23*, 1443–1484.

(5) Qu, L.; Shi, G.; Chen, F.; Zhang, J. Electrochemical Growth of Polypyrrole Microcontainers. *Macromolecules* **2003**, *36*, 1063–1067.

(6) Gurunathan, K.; Murugan, A. V.; Marimuthu, R.; Mulik, U. P.; Amalnerkar, D. P. Electrochemically Synthesised Conducting Polymeric Materials for Applications towards Technology in Electronics, Optoelectronics and Energy Storage Devices. *Mater. Chem. Phys.* **1999**, *61*, 173–191.

(7) Chen, S.-M. Preparation, Characterization, and Electrocatalytic Oxidation Properties of Iron, Cobalt, Nickel, and Indium Hexacyanoferrate. *J. Electroanal. Chem.* **2002**, *521*, 29–52.

(8) Ma, H.; Chen, Y.; Li, X.; Li, B.; Ma, H.; Chen, Y.; Li, X.; Li, B. Advanced Applications and Challenges of Electropolymerized Conjugated Microporous Polymer Films. *Adv. Funct. Mater.* **2021**, *31*, 2101861.

(9) Wang, B. H.; Ma, Y. G.; Cao, Y. A Brief Introduction to Organic Electrodeposition and a Review of the Fabrication of OLEDs Based on Electrodeposition Technology. *Chin. J. Polym. Sci.* **2023**, *41*, 621–639.

(10) Choi, E. J.; Drago, N. P.; Humphrey, N. J.; Van Houten, J.; Ahn, J.; Lee, J.; Kim, I. D.; Ogata, A. F.; Penner, R. M. Electrodeposition-Enabled, Electrically-Transduced Sensors and Biosensors. *Mater. Today* **2023**, *62*, 129–150.

(11) Viswanathan, B.; Armstrong, A. R.; Okhay, O.; Tkach, A. Polyaniline—Graphene Electrodes Prepared by Electropolymerization for High-Performance Capacitive Electrodes: A Brief Review. *Batteries* **2022**, *8*, 191.

(12) Holze, R. Conjugated Molecules and Polymers in Secondary Batteries: A Perspective. *Molecules* **2022**, *27*, 546.

(13) Zhang, H.; Wang, X.; Ma, H.; Xue, M. Recent Progresses on Applications of Conducting Polymers for Modifying Electrode of Rechargeable Batteries. *Adv. Energy Sustainability Res.* **2021**, *2*, 2100088.

(14) Shao, J. Y.; Zhong, Y. W. Toward Stable and Efficient Solar Cells with Electropolymerized Films. *ACS Sustainable Chem. Eng.* **2022**, *10*, 13555–13567.

(15) Cansu Ergun, E. G.; Bezgin Carbas, B. Electrochromic Copolymers of 2,5-Dithienyl-N-Substituted-Pyrrole (SNS) Derivatives with EDOT: Properties and Electrochromic Device Applications. *Mater. Today Commun.* **2022**, *32*, 103888.

(16) Zhang, Y.; Lv, H.; Zhang, Z.; Wang, L.; Wu, X.; Xu, H. Stable Unbiased Photo-Electrochemical Overall Water Splitting Exceeding 3% Efficiency via Covalent Triazine Framework/Metal Oxide Hybrid Photoelectrodes. *Adv. Mater.* **2021**, *33*, 2008264.

(17) Runsewe, D.; Betancourt, T.; Irvin, J. A. Biomedical Application of Electroactive Polymers in Electrochemical Sensors: A Review. *Materials* **2019**, *12*, 2629.

(18) Xiao, Z.-Y.; Zhao, X.; Jiang, X.-K.; Li, Z.-T. Tunable Coordinative Assembly of a Disc-Like Molecule and Metal Ions: From Mirospheres to Microtubes and Microrods. *Chem. Mater.* **2011**, *23*, 1505–1511.

(19) Banfi, S.; Carlucci, L.; Caruso, E.; Ciani, G.; Proserpio, D. M. Using Long Bis(4-Pyridyl) Ligands Designed for the Self-Assembly of Coordination Frameworks and Architectures. *J. Chem. Soc., Dalton Trans.* **2002**, No. 13, 2714–2721.

(20) Jena, S. R.; Mandal, T.; Choudhury, J. Metal-Terpyridine Assembled Functional Materials for Electrochromic, Catalytic and Environmental Applications. *Chem. Rec.* **2022**, *22*, e202200165.

(21) Altman, M.; D. Shukla, A.; Zubkov, T.; Evmenenko, G.; Dutta, P.; E. van der Boom, M. Controlling Structure from the Bottom-Up: Structural and Optical Properties of Layer-by-Layer Assembled Palladium Coordination-Based Multilayers. *J. Am. Chem. Soc.* **2006**, *128*, 7374–7382.

(22) Kohli, P.; J. Blanchard, G. Design and Demonstration of Hybrid Multilayer Structures: Layer-by-Layer Mixed Covalent and Ionic Interlayer Linking Chemistry. *Langmuir* **2000**, *16*, 8518–8524.

(23) Shekhah, O.; Wang, H.; Strunskus, T.; Cyganik, P.; Zacher, D.; Fischer, R.; Wöll, C. Layer-by-Layer Growth of Oriented Metal Organic Polymers on a Functionalized Organic Surface. *Langmuir* **2007**, *23*, 7440–7442.

(24) Zhu, X. J.; Holliday, B. J. Electropolymerization of a Ruthenium(II) Bis(Pyrazolyl)Pyridine Complex to Form a Novel Ru-Containing Conducting Metallopolymer. *Macromol. Rapid Commun.* **2010**, *31*, 904–909.

(25) Higgins, S. J. Conjugated Polymers Incorporating Pendant Functional Groups—Synthesis and Characterisation. *Chem. Soc. Rev.* **1997**, *26*, 247–257.

(26) Welterlich, I.; Tieke, B. Conjugated Polymer with Benzimidazolylpyridine Ligands in the Side Chain: Metal Ion Coordination and Coordinative Self-Assembly into Fluorescent Ultrathin Films. *Macromolecules* **2011**, *44*, 4194–4203.

(27) Tieke, B. Coordinative Supramolecular Assembly of Electrochromic Thin Films. *Curr. Opin. Colloid Interface Sci.* **2011**, *16*, 499–507.

(28) Maier, A.; Cheng, K.; Savych, J.; Tieke, B. Double-Electrochromic Coordination Polymer Network Films. *ACS Appl. Mater. Interfaces* **2011**, *3*, 2710–2718.

(29) Pan, Y.; Tong, B.; Shi, J.; Zhao, W.; Shen, J.; Zhi, J.; Dong, Y. Fabrication, Characterization, and Optoelectronic Properties of Layer-by-Layer Films Based on Terpyridine-Modified MWCNTs and Ruthenium(III) Ions. *J. Phys. Chem. C* **2010**, *114*, 8040–8047.

(30) Liu, J.; Chen, M.; Qian, D.-J. Copper(II)-Mediated Layer-by-Layer Assembly of Viologenthiol-Functionalized Carbon Nanotube Hybrid Multilayers: Preparation, Characterization, Morphology, and Electrochemical Properties. *Langmuir* **2012**, *28*, 9496–9505.

(31) Zacher, D.; Shekhah, O.; Wöll, C.; Fischer, R. A. Thin Films of Metal–Organic Frameworks. *Chem. Soc. Rev.* **2009**, *38*, 1418–1429.

(32) Zacher, D.; Schmid, R.; Wöll, C.; Fischer, R. A. Surface Chemistry of Metal–Organic Frameworks at the Liquid–Solid Interface. *Angew. Chem. Int. Ed.* **2011**, *50*, 176–199.

(33) Wang, Y.; Li, M. Controlled Electropolymerization Based on Self-Dimerizations of Monomers. *Curr. Opin. Electrochem.* **2022**, *33*, 100952.

(34) Friebe, C.; Hager, M. D.; Winter, A.; Schubert, U. S. Metal-Containing Polymers via Electropolymerization. *Adv. Mater.* **2012**, *24*, 332–345.

(35) Zhong, Y.-W.; Yao, C.-J.; Nie, H.-J. Electropolymerized Films of Vinyl-Substituted Polypyridine Complexes: Synthesis, Characterization, and Applications. *Coord. Chem. Rev.* **2013**, *257*, 1357–1372.

(36) Hanabusa, K.; Nakamura, A.; Koyama, T.; Shirai, H. Electropolymerization and Characterization of Terpyridinyl Iron (II) and Ruthenium (II) Complexes. *Polym. Int.* **1994**, *35*, 231–238.

(37) Toma, S. H.; Santos, J. J.; Velho, R. G.; Nakamura, M.; Toma, H. E.; Araki, K. Electrochemically Activated Coordenative Assembly of a Triruthenium Cluster Metallopolymer. *Electrochim. Acta* **2012**, *66*, 287–294.

(38) Chiper, M.; Meier, M. A. R.; Kranenburg, J. M.; Schubert, U. S. New Insights into Nickel(II), Iron(II), and Cobalt(II) Bis-Complex-Based Metallo-Supramolecular Polymers. *Macromol. Chem. Phys.* **2007**, *208*, 679–689.

(39) Hu, C.-W.; Sato, T.; Zhang, J.; Moriyama, S.; Higuchi, M. Multi-Colour Electrochromic Properties of Fe/Ru-Based Bimetallo-Supramolecular Polymers. *J. Mater. Chem. C* **2013**, *1*, 3408–3413.

(40) Maeda, H.; Sakamoto, R.; Nishimori, Y.; Sendo, J.; Toshimitsu, F.; Yamanoi, Y.; Nishihara, H. Bottom-Up Fabrication of Redox-Active Metal Complex Oligomer Wires on an H-Terminated Si(111) Surface. *Chem. Commun.* **2011**, *47*, 8644–8646.

Table of Contents